ORIGINAL ARTICLE

Cerebellar ataxia induced by 3-AP affects immunological function

Yong-Ying Jiang, Bei-Bei Cao, Xiao-Qin Wang, Yu-Ping Peng, Yi-Hua Qiu

Department of Physiology, School of Medicine, and Co-innovation Center of Neuroregeneration, Nantong University, Nantong, Jiangsu Province, China

Correspondence to:	Yu-Ping Peng
	Department of Physiology, School of Medicine, Nantong University
	19 Qixiu Road, Nantong, Jiangsu Province, 226001, China.
	TEL: +86-513-85051714; E-MAIL: yppeng@ntu.edu.cn

Yi-Hua Qiu
Department of Physiology, School of Medicine, Nantong University
19 Qixiu Road, Nantong, Jiangsu Province, 226001, China.
TEL: +86-513-85051723; E-MAIL: yhqiu@ntu.edu.cn

Abstract

OBJECTIVE: We previously showed that the cerebellum modulates the immune system. Here we determined whether cerebellar ataxia alters immunological function to further demonstrate an involvement of the cerebellum in immune modulation.

METHODS: Neurotoxin 3-acetylpyridine (3-AP) was intraperitoneally injected in rats to induce cerebellar ataxia. Behavior and motor coordination were tested on day 7 following 3-AP injection. Nissl staining and high-performance liquid chromatography (HPLC) were used to determine neuronal loss and neurotransmitter contents, respectively, in all the three cerebellar nuclei, fastigial nucleus (FN), interposed nucleus (IN) and dentate nucleus (DN). T and B lymphocyte differentiation and function were measured by flow cytometry, Western blot and ELISA.

RESULTS: 3-AP induced motor discoordination and locomotor reduction. In all the three cerebellar nuclei, FN, IN and DN, there was a neuronal loss and a decrease in contents of glutamate and GABA (but not glycine) after 3-AP injection. Importantly, CD4+ T cells, but not CD8+ T cells, were increased by the 3-AP treatment. Moreover, interferon (IFN)-γ-producing cells and interleukin (IL)-17-producing cells were decreased in cerebellar ataxia rats, but IL-4-producing cells and CD25-expressing cells were increased. Expression of the T helper (Th)1- and Th17-related cytokines, IFN-γ, IL-2, IL-17 and IL-22, was downregulated in CD4+ cells in cerebellar ataxia rats, while expression of the Th2 and regulatory T (Treg)-related cytokines, IL-4, IL-5, IL-10 and transforming growth factor (TGF)-β, was upregulated. Furthermore, B lymphocyte number and anti-bovine serum albumin (BSA) IgM and IgG antibody levels were elevated in cerebellar ataxia.

CONCLUSION: Cerebellar ataxia alters cellular and humoral immunity.

INTRODUCTION

Cerebellar ataxias are a group of neurodegenerative disorders characterized by progressive degeneration of the cerebellum and often accompanied by a variety of neurological and other systemic symptoms (Brusse *et al.* 2007; Marmolino & Manto 2010). Since the cerebellum is predominantly a motor control center, its role in regulating other systems is less clear. In recent decade, the cerebellum has been found to regulate non-somatic activities (Wen *et al.* 2004; Zhu & Wang 2008; Rosenberger *et al.* 2013). Lesions to cerebellar nuclei result in dysfunction of visceral activities (Mori *et al.* 2005; Zhu *et al.* 2012). Interestingly, immune system function is also modulated by the cerebellum (Green-Johnson *et al.* 1995; Ghoshal *et al.* 1998). Our previous work has shown that the two cerebellar nuclei, fastigial nucleus (FN) and interposed nucleus (IN), have opposite immunoregulatory effects, strongly showing an involvement of the cerebellum in modulation of the immune system (Peng *et al.* 2005, 2006). Accordingly, we hypothesized that cerebellar ataxia may affect immunological function. Recently, a report has presented that patients with ataxia telangiectasia, a multisystem DNA-repair disorder, have a highly variable immunodeficiency that correlates with disturbances in B- and T-cell homeostasis (Driessen *et al.* 2013). In addition, in some patients with sporadic cerebellar ataxia of unknown origin, there is probably a heightened autoimmune background (Sivera *et al.* 2012). These reports suggest a relationship between ataxia diseases and immune disorders. Nevertheless, it is not known whether cerebellar ataxia directly results in immunological changes. Here, we employed a rat model of cerebellar ataxia by intraperitoneal injection of 3-acetylpyridine (3-AP) to determine changes in adaptive immune responses.

Neurotoxin 3-AP, an antimetabolite of nicotinamide, has been shown to produce highly selective lesion of the inferior olive nucleus (Llinás *et al.* 1975; Fernandez *et al.* 1998; Sierra *et al.* 2003; Janahmadi *et al.* 2009; Abbasi *et al.* 2013). Neurons in the inferior olive nucleus send axons, termed climbing fibers, up to cerebellar cortex, where the climbing fibers form synapses on Purkinje cells, and in turn the Purkinje cells project axons to all the three cerebellar nuclei, FN, IN and dentate nucleus (DN). Neurons in the cerebellar nuclei finally export information out of the cerebellum to the thalamus, cerebral cortex, brainstem and hypothalamus to modulate motor and visceral activities (Desclin & Escubi 1974; Aoki & Sugihara 2012). In addition, a single inferior olive axon in rats branches several climbing fibers that terminate in extensive regions of the cerebellum including molecular layer, granular layer and the three nuclei to modulate cerebellar activities (Sugihara *et al.* 1999, 2001; Sugihara 2006, 2011; Aoki & Sugihara 2012). Therefore, destruction of the nerve fibers innervating the cerebellum by 3-AP can induce cerebellar ataxia.

Adaptive immune responses are executed by T and B lymphocytes. T lymphocytes are responsible for cellular immune response and B lymphocytes are involved in humoral immune response. Based on different surface molecules, T cells are divided into $CD4^+$ and $CD8^+$ cells. $CD4^+$ cells are subdivided into the four subpopulations, T helper (Th)1, Th2, Th17 and regulatory T (Treg) cells. Th1 and Th17 cells are pro-inflammatory by secreting inflammatory cytokines such as interferon (IFN)-γ, interleukin (IL)-2, IL-17 and IL-22. Th2 and Treg cells are anti-inflammatory by releasing immunosuppressive cytokines such as IL-4, IL-5, IL-10 and transforming growth factor (TGF)-β. In this study, the cellular and humoral immune responses were evaluated in cerebellar ataxia model rats to determine an involvement of immunological changes in cerebellar ataxia.

MATERIALS AND METHODS

Animals and preparation of cerebellar ataxia

All studies were conducted using male Sprague-Dawley rats (Center of Experimental Animals, Nantong University, China) with an initial weight of 220–240 g. Rats were kept on a 22 °C and 12-hour light/dark cycle room, with free access to food and water. Housing and experimental procedures were carried out in accordance with the policy guidelines of the National Institutes of Health Guide for the Care and Use of Laboratory Animals (NIH Publications No. 80-23) revised 1996, and approved by Nantong University Committee for Care and Use of Laboratory Animals. Rats were randomly divided into the three groups, intact, saline and 3-AP, with 15 for each group. For preparation of cerebellar ataxia model, rats were intraperitoneally injected with 3-AP (65 mg/kg body weight). Behavioral and motor coordination changes of rats were observed each day after the 3-AP injection until the rats were sacrificed. Immunological and other data were determined on day 7 following the 3-AP injection.

Behavioral and motor coordination tests

Behavior and motor coordination of rats were determined by rota-rod, balance beam and open-field tests. For rota-rod test, rats were placed on a rotating rod with an increasing acceleration (4–40 rpm drive speed) in a rota-rod apparatus (Ugo Basile, Italy). The head of rat directed against the direction of rotation so that the rat progressed forward to avoid falling. The time keeping on the rotating rod was recorded as latency of rat falling.

Balance beam is a rod with 160 cm in length and 2.5 cm in diameter, which is suspended 90 cm above a cushion to protect the fallen animals from injury and 50 cm from a wall. A plastic platform (7 cm × 4 cm) is set at one end of the rod as the start, and a black plastic box (15 cm × 15 cm × 8 cm) is at the other end of the rod as a nest for motivating the animals' crossing along the beam. The time taken to traverse the beam

was recorded. If rats failed to pass through the beam, the time was set as 60 s.

A square open field (50 cm × 50 cm × 50 cm) consists of a black plastic platform and a white plastic barrier enclosed the arena. The floor of the arena is divided into 9 identical squares. A video camera is suspended over the arena to automatically record activity of animals. Each rat was carefully placed in the center of the open field, and number of squares crossed by the rat and velocity of movement during a 2-min period were quantified as locomotor activity.

Nissl staining

Rats were perfused with 4% paraformaldehyde (pH 7.4) after anesthetized. The 30 μm-thick coronal sections of the cerebellum were cut in a cryostat (Leica cm 1900-1-1, Germany) after the brains were post-fixed in the same fixative for 2–4 h at 4 °C. To ensure cerebellar sections were matched between groups, anatomical landmarks provided by the brain atlas (Paxinos & Watson 2007) were used. The sections were mounted on polylysine-coated slides, dried overnight, rehydrated in distilled water, and then submerged in 1% cresyl violet for about 20 min until the desired depth of staining was achieved. After rinsed in distilled water and dehydrated in graded serried of ethanol, the sections were immersed in xylene, mounted in neutral balsam, and then coverslipped. Nissl bodies in the three cerebellar nuclei, FN, IN and DN, were observed to determine neuronal loss.

High-performance liquid chromatography (HPLC) assay for determination of amino acids

The experimental procedures were similar to those described in our previous reports (Cao et al. 2013; Xu et al. 2014). The three cerebellar nuclei, FN, IN and DN, were removed on ice, respectively. The tissues were respectively homogenized in 0.5 M perchloric acid (1:10, w/v) and then centrifuged at $300 \times g$ for 15 min at 4 °C. For measurement of amino acid neurotransmitters including glutamate, glycine and γ-aminobutyric acid (GABA), 10 μl supernatant of each sample from the FN, IN or DN was injected into HPLC equipment supplemented with a fluorescent detection (Waters, USA) and with an amino acid analysis column (AccQ TagTM, 3.9 × 150 mm, 4 μm beads, Waters, USA). Mobile phase was pumped at a flow rate of 1.0 ml/min. A gradient elution was used to separate the mixture of the amino acids. Fluorometric detection was performed at an excitation wavelength of 250 nm and an emission wavelength of 395 nm.

Flow cytometric assay of T and B lymphocyte percentages in peripheral blood mononuclear cells (PBMCs)

A minimum of 2 ml of whole blood was collected in an EDTA-containing tube by endocardiac puncture of rats that had been anesthetized with pentobarbital. PBMCs were isolated by Ficoll-Hypaque centrifugation ($356 \times g$

for 20 min). The cells were incubated with anti-rat CD3-PE antibody (eBioscience, USA; 0.25 μg in 100 μl PBS), anti-rat CD45RA-FITC antibody (eBioscience, USA; 1 μg in 100 μl PBS), anti-rat CD4-APC antibody (eBioscience, USA; 0.25 μg in 100 μl PBS), or anti-rat CD8-FITC antibody (eBioscience, USA; 0.25 μg in 100 μl PBS) for 30 min at room temperature protecting from light. After washing, the cells were resuspended in 500 μl of 0.01 M PBS. Analyses were performed with a FACSArray flow cytometer (BD Biosciences, USA) and data were analyzed using CellQuest software (BD Biosciences, USA).

Flow cytometry for CD4+ cell differentiation

The mesenteric lymph nodes were harvested aseptically from the anesthetized rats by celiotomy. CD4+ T lymphocytes in the mesenteric lymph nodes were purified with magnetic beads (Miltenyi Biotec, Germany) and incubated with plate-bound anti-CD3 (BD PharMingen, USA; 25 μg/ml) and soluble anti-rat CD28 (BD PharMingen, USA; 2 μg/ml) for 72 h. The cells were stained during 30 min at 4 °C with combination of the surface marker FITC-labeled anti-CD25 (BD PharMingen, USA). Subsequently, for the intracellular cytokine staining, the cells were stimulated with phorbol 12-myristate13-acetate (Sigma-Aldrich, USA; 50 ng/ml) and ionomycin (Sigma-Aldrich, USA; 1 μM) in the presence of GolgiStop (BD PharMingen, USA) at the concentration recommended by the manufacturer for 5 h at 37 °C in a 5% CO_2 humidified atmosphere. The cells were fixed and permeabilized for 20 min at 4 °C in 250 μl Perm/Fix buffer (BD PharMingen, USA). After being washed in Perm/Wash buffer (BD PharMingen, USA), the cells were stained with PE-conjugated anti-IFN-γ (BioLegend, USA), PE-labeled anti-IL-4 (BioLegend, USA), or PE-labeled anti-IL-17 (eBioscience, USA) for 30 min at 4 °C. All samples were analyzed using a FACS Calibur flow cytometer with CellQuest software (BD Bioscience, USA).

Real-time PCR analysis

Total RNA of CD4+ T lymphocytes that were isolated from the mesenteric lymph nodes as described above was extracted with Trizol reagent (Invitrogen, USA) according to the manufacturer's instructions. The 2 μg of total RNA was reversely transcribed in a 20 μl reaction for cDNA synthesis with murine myelomonocytic lymphoma virus reverse transcriptase (Promega, USA). The single-stranded cDNA was then amplified by real-time quantitative PCR. Each 20 μl of reaction mixture contained 1 μl of cDNA, 2 μl PCR buffer, 3.0 mM $MgCl_2$, 0.2 mM of each dNTP, 0.2 μM of each pair of oligonucleotide primers, and 1 U Taq DNA polymerase. Reaction procedures were as follows: an initial step at 95 °C for 5 min, 40 cycles of 94 °C for 15 s, 62 °C for 20 s, and 72 °C for 20 s. The data were collected using the instrument's software (Rotor-Gene software, version 6.0) and relative quantification was performed using the compara-

tive threshold (CT) method after determining the CT values for reference (β-actin) and target genes (IFN-γ, IL-2, IL-4, IL-5, TGF-β, IL-10, IL-17 and IL-22) in each sample set according to the $2^{-\Delta\Delta Ct}$ method, as described by the manufacturer (User Bulletin). Changes in mRNA expression levels were calculated after normalization to β-actin. The primer sequences of the target genes are listed in Table 1.

Western blot analysis

CD4+ T lymphocytes were homogenized in an sodium dodecyl sulfate (SDS) sample buffer that contained a mixture of proteinase inhibitors and then the supernatants were collected by centrifuging at 4°C at $13,200 \times g$ for 15 min. The supernatants were mixed with loading buffer, which was boiled for 10 min. The proteins were separated by 10% sodium dodecyl sulfate-polyacrylamide gel electrophoresis and transferred to a polyvinylidene difluoride membrane (Pall, USA) using an electroblotting apparatus (Bio-Rad, USA). The membranes were blocked for 1 h in Tris-buffered saline containing 0.1% Tween-20 and 5% dry milk and then incubated at 4°C overnight with the primary antibodies to IFN-γ (Santa Cruz Biotechnology, Inc., USA; 1:200), IL-2 (Santa Cruz Biotechnology, Inc., USA; 1:100), IL-4 (R&D Systems, Germany; 1:500), IL-5 (Santa Cruz Biotechnology, Inc., USA; 1:200), TGF-β (Santa Cruz Biotechnology, Inc., USA; 1:400), IL-10 (Santa Cruz Biotechnology, Inc., USA; 1:200), IL-17 (Santa Cruz Biotechnology, Inc., USA; 1:100), or IL-22 (Santa Cruz Biotechnology, Inc., USA; 1:100). The membranes were probed at 4°C overnight and incubated with IRDye 800-conjugated goat anti-rabbit IgG (Rockland Immunochemicals, Inc., USA; 1:5,000), IRDye 800-conjugated goat anti-mouse IgG (Rockland Immunochemicals, Inc., USA; 1:5,000), or IRDye 800-conjugated donkey anti-goat IgG (LI-COR Inc, USA; 1:5,000) for 1 h at room temperature, followed by visualization by Odyssey laser scanning system (LI-COR Inc, USA). The blots were re-probed with monoclonal mouse anti-β-actin antibody (Sigma-Aldrich, USA; 1:5,000) and reacted with IRDye 800-conjugated goat anti-mouse IgG (Rockland Immunochemicals, Inc., USA; 1:5,000) to confirm equal protein loading. The molecular weight and relative quantity of each protein band were determined by an image analysis system (Odyssey 3.0 software).

Trypan blue staining of lymphocytes

To show whether 3-AP has direct toxicity to lymphocytes, we detected the viability of lymphocytes using Trypan blue staining. The mesenteric lymph nodes were aseptically harvested by celiotomy from the pentobarbital-anesthetized rats (55 mg/kg, i.p.). Lymphocytes were obtained by gently squeezing the lymph nodes and by passing the tissue through a 200-μm nylon mesh screen. The lymphocytes were washed twice with RPMI 1640 culture medium (Gibco, USA) and erythrocytes were lysed by sterilized distilled water. The lymphocytes were then resuspended in complete culture medium that consisted of RPMI 1640 medium, 10% heat-inactivated foetal calf serum, 2.5×10^{-2} M HEPES (Sigma-Aldrich, USA), 1×10^{-3} M sodium pyruvate, 5×10^{-5} M β-mercaptoethanol and antibiotics (100 U/ml penicillin, 100 U/ml streptomycin) at a concentration of 3×10^6 cells/ml. 3-AP was added to the cultures at the three concentrations, 0.1 mM, 1 mM and 10 mM, followed by an incubation in 5% CO_2 at 37°C for 48 h. Trypan blue (0.4%) was mixed with lymphocyte suspensions at a ratio of 1:1, which was placed in room temperature for 2–3 min. The dead cells were dyed blue, and living cells remained colorless. The cell viability was expressed as percentage of living cells in total cells.

Methyl-thiazole-tetrazolium (MTT) assay for lymphocyte proliferation

The MTT assay was also used to determine if 3-AP is toxic to lymphocytes. The isolation of lymphocytes was the same as described in trypan blue staining. The lymphocytes were then resuspended in the complete culture medium at a concentration of 1×10^6 cells/ml. Concanavalin A (Con A, 5 mg/ml) and 3-AP (0.1, 1 or 10 mM) were simultaneously added to the cultures, which were incubated at 37°C in 5% CO_2 for 48 h. MTT (Sigma-Aldrich, USA) solution of 5 mg/ml was added to the cultures (10 ml MTT solution per 100 ml medium), followed by an incubation in 5% CO_2 at 37°C for 4 h. SDS (20%) containing 50% N'N-dimethylformamide was added to the cultures, which were incubated for 12 h at 37°C in 5% CO_2. Lastly, the optical density (OD) was read on a multi-mode microplate reader (Bio Tek, USA) using a test wavelength of 570 nm.

Enzyme-linked immunosorbent assay (ELISA) for IgM and IgG antibody levels in serum

Rats were intraperitoneally injected with bovine serum albumin (BSA) twice (day 3 before and day 2 after 3-AP treatment) to induce production of specific anti-BSA IgM and IgG antibodies. Blood was taken from right ventricle on the fifth day and on the tenth day after the

Tab. 1. Sequences of PCR primers.

Gene	Sense primer	Antisense primer
IL-2	5'-CCATGATGCTCACGTTTAAATTTT-3'	5'-CATTTTCCAGGCACTGAAGATG-3'
IFN-γ	5'-GCCCTCTCTGGCTGTTACTG-3'	5'-TACCGTCCTTTTGCCAGTTC-3'
IL-4	5'-ACCTTGCTGTCACCCTGTTCT-3'	5'-CTCTCTCAGAGGGCTGTCGTTA-3'
IL-5	5'-CAGTGGTGAAAGAGACCTTGATACAG-3'	5'-GAAGCCTCATCGTCTCATTGC-3'
IL-10	5'-TGCCTTCAGTCAAGTGAAGAC-3'	5'-AAACTCATTCATGGCCTTGTA-3'
TGF-β	5'-TGGAAATCAATGGGATCAGTC-3'	5'-GTAGTTGGTATCCAGGGCTC-3'
IL-17	5'-TGGACTCTGAGCCGCAATG-3'	5'-GGCGGACAATAGAGGAAACG-3'
IL-22	5'-AGCGGTGATGACCAGAACA-3'	5'-CTCAGGGACATAAACAGCAGA-3'
β-actin	5'-CGTTGACATCCGTAAAGACC-3'	5'-TAGAGCCACCAATCCACAC-3'

Yong-Ying Jiang, Bei-Bei Cao, Xiao-Qin Wang, Yu-Ping Peng, Yi-Hua Qiu

first injection of BSA for measurement of IgM and IgG levels, respectively. The serum was collected by centrifugation at $900 \times g$ for 20 min. A 96-well microtiter plate was coated with BSA membrane and stored at 4°C for at least 16 h. After washing with 0.05% Tween 20 (Sigma-Aldrich, USA), the plate was blocked with blocking buffer for 1 h to avoid non-specific binding. Diluted serum samples (1:200 in 0.01 M PBS) were added to the wells (100 μl/well), which were incubated at 37°C for 3 h. After washed, the samples were incubated with peroxidase-conjugated goat anti-rat IgG (Sigma-Aldrich, USA; 1:3,000) for 2 h at 37°C. After washing, 3,3',5,5'-tetramethylbenzidine (Sigma-Aldrich, USA) was added to each well, which was incubated for 10 min. The reaction was stopped with stop buffer. Absorbance was determined with a multi-mode microplate reader (Bio Tek, USA) at 450 nm.

Statistical analysis

Data were expressed as means ± standard deviation (M ± SD). Statistical analyses were performed with the Statistics Package for Social Science (SPSS, 19.0). The data were subjected to the one-way analysis of variance (ANOVA), followed by Student-Newman-Keul's test to compare the data of all groups relative to each other. Differences were considered statistically significant at $p < 0.05$.

RESULTS

3-AP injection induces behavioral and motor coordination impairments

A behavioral and motor change was observed from day 1 to day 7 after intraperitoneal injection of 3-AP. Compared with intact or saline-injected rats, animals with 3-AP injection manifested attention reduction, activeness weakness, body tremor, movement unbalance, and failure of tail movement. The manifestations were progressively exacerbated over time after 3-AP injection. In addition, 3-AP injection significantly decreased time of rats keeping on rota-rod relative to intact or saline controls (Figure 1A). The animals with 3-AP injection failed to pass through balance beam and hence the time (recorded as 60 s) was significantly longer than that (about 10 s) of

intact or saline animals (Figure 1B). The 3-AP-injected rats also reduced number of moving through grids and speed of movement in open-field test (Figure 1C).

3-AP injection causes neuronal loss and decreases contents of amino acid neurotransmitters in cerebellar nuclei

Nissl staining of cerebellar sections showed that Nissl bodies in the three cerebellar nuclei, FN, IN and DN, remarkably lost on the 7th day after 3-AP injection with respect to those of intact or saline controls (Figure 2A). Simultaneously, the 3-AP injection reduced contents of glutamate and GABA, but not glycine, in all the three cerebellar nuclei, FN, IN and DN, compared with intact or saline controls (Figure 2B).

Cerebellar ataxia model rats have a CD4± cell differential and functional shift from Th1 and Th17 cells toward Th2 and Treg cells

CD3+CD4+ cells (a subset of T lymphocytes) include four subpopulations, Th1 cells that produce cytokine IFN-γ, Th2 cells that produce IL-4, Th17 cells that produce IL-17, and Treg cells that express CD25. Percentage of CD3+CD4+ cells in PBMCs was elevated in 3-AP-induced cerebellar ataxia rats, although neither CD3+CD45RA- cells (total T lymphocytes) nor CD3+CD8+ cells (another subset of T cells) were significantly altered, compared with those of intact or saline animals (Figure 3A).

To show differentiation levels of CD4+ T cells towards the four subpopulations, we determined percentages of specific cytokine-producing cells in CD4+ T cells that were purified and stimulated with anti-CD3/CD28 antibodies to induce production of the cytokines. Compared with intact or saline rats, cerebellar ataxia model rats were decreased in percentages of IFN-γ- or
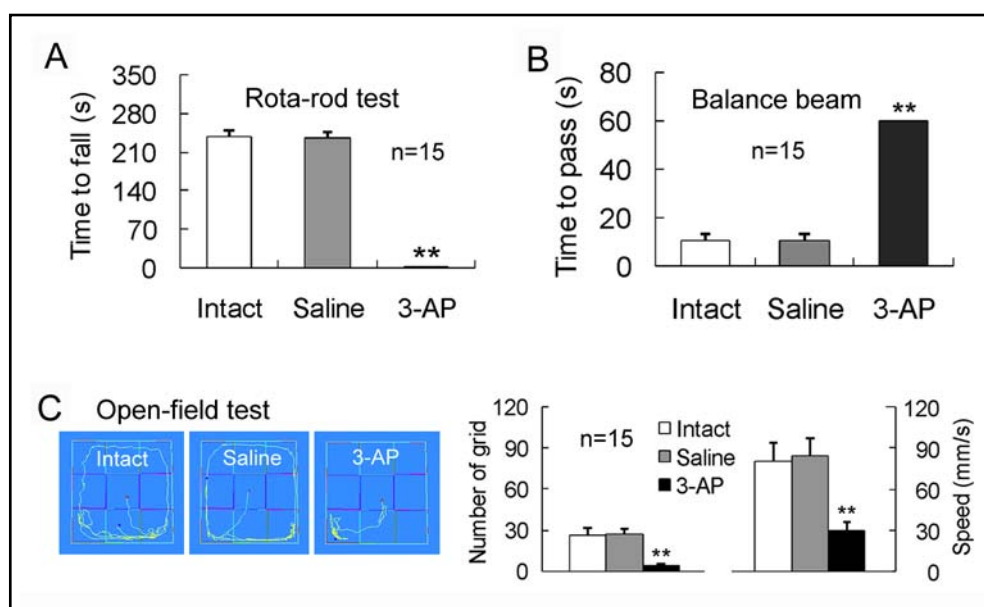

Fig. 1. 3-AP intraperitoneal injection in rats induces behavioral and motor impairments. Motor coordination, movement balance and locomotor activity of rats were evaluated by rota-rod (**A**), balance beam (**B**) and open-field (**C**) tests, respectively. **p<0.01, compared with intact or saline rats.
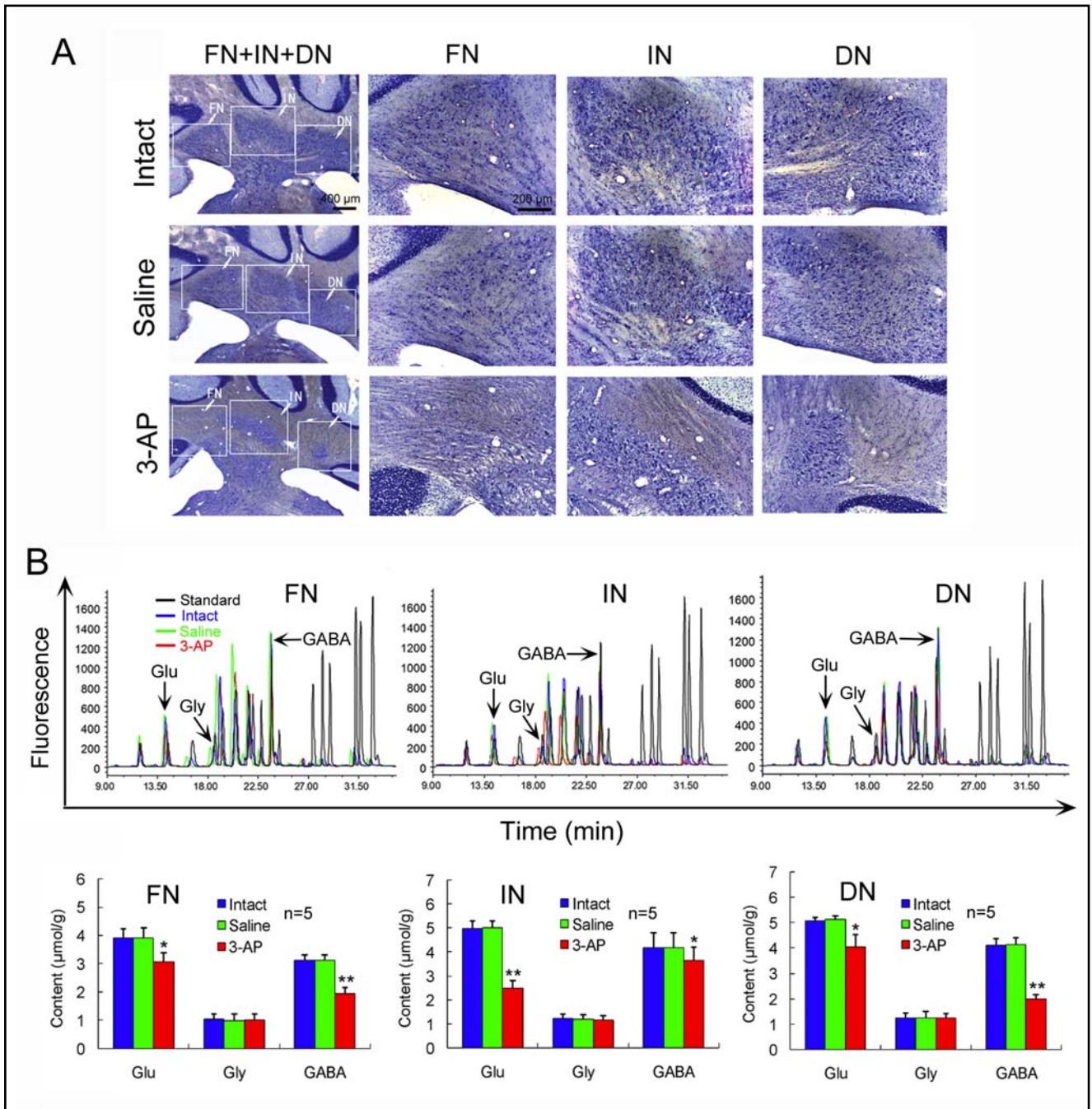
Fig. 2. Neuronal loss and amino acid neurotransmitter decrease in cerebellar nuclei by 3-AP treatment. (A) Illustration of three cerebellar nuclei on Nissl-stained sections. On these sections of intact and saline-treated rats, Nissl bodies, which exist in the plasma of neuronal soma and are stained with violet, are clearly seen in the three cerebellar nuclei, FN, IN and DN. However, on the slices of the 3-AP-injected rat, Nissl bodies remarkably decrease in the three cerebellar nuclei, showing a loss of cell bodies of neurons. (B) Contents of amino acid neurotransmitters in cerebellar nuclei. The upper panel in (B) represents typical peaks of the amino acid neurotransmitters, glutamate (Glu), GABA and glycine (Gly), in the three cerebellar nuclei, FN, IN and DN, which were determined by HPLC. The lower panel in (**B**) is a statistical histogram. *$p<0.05$, **$p<0.01$, compared with intact or saline-injected rats.

IL-17-producing cells but increased in percentages of IL-4-producing or CD25-expressing cells in CD4+ T cells (Figure 3B).

Function of the various subpopulations of CD4+ T cells is mainly reflected by levels of cytokines specifically produced by the cells. IFN-γ and IL-2, the Th1-related cytokines, and IL-17 and IL-22, the Th17-related cyto-kines, were downregulated at both mRNA and protein expression levels in CD4+ T cells in cerebellar ataxia rats relative to those of intact or saline animals (Figure 4A, B). In contrast, IL-4 and IL-5, the Th2-related cyto-kines, and TGF-β and IL-10, the Treg-related cytokines, were upregulated in CD4+ T cells in cerebellar ataxia rats (Figure 4A, B).
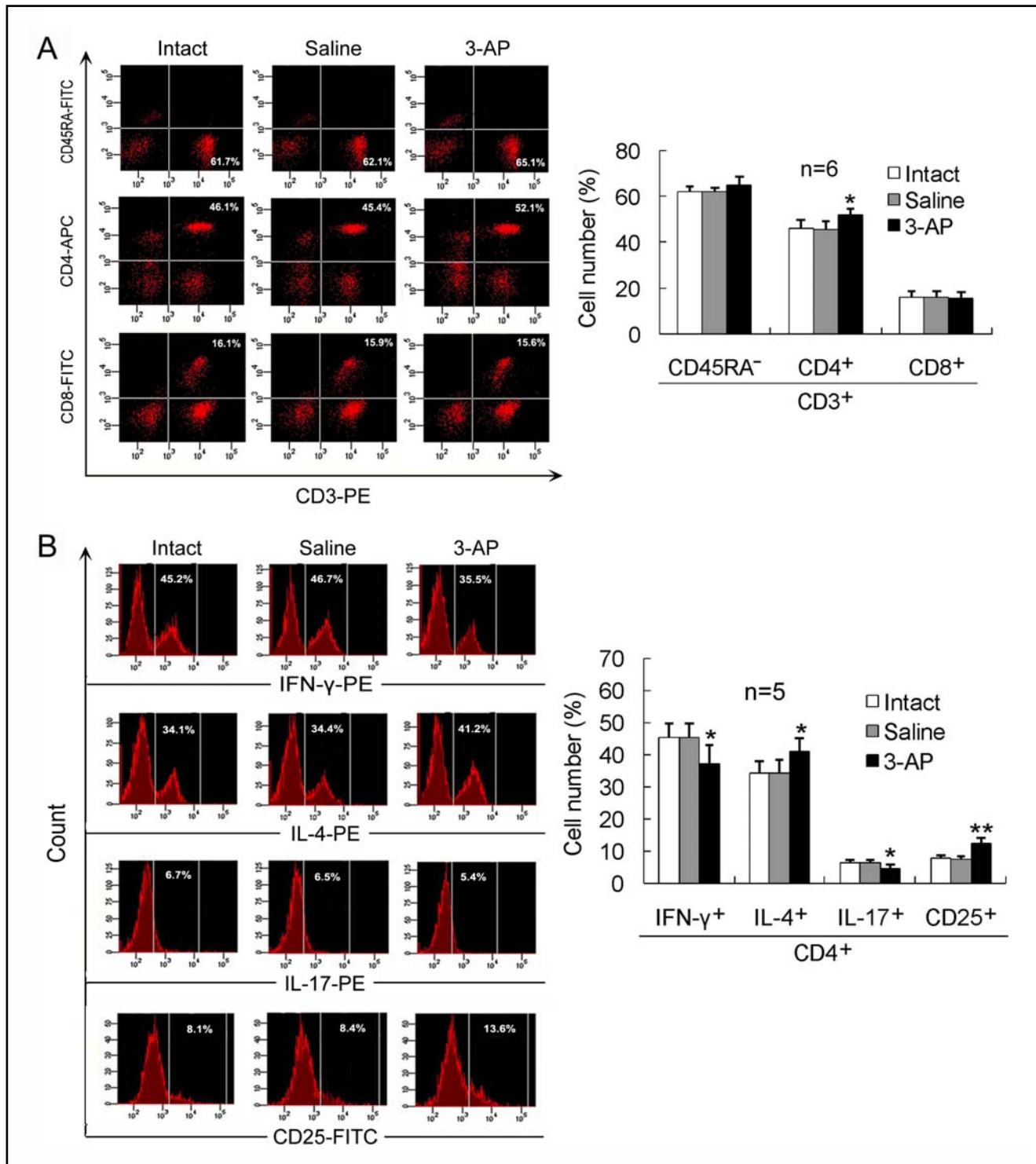
Fig. 3. Changes in number and differentiation of T lymphocytes in cerebellar ataxia model rats. (**A**) Percentages of T lymphocytes (CD3+CD45RA−) and T cell subsets (CD3+CD4+ and CD3+CD8+) in PBMCs. (**B**) Percentages of different cytokine-producing cells in CD4+ cells. It shows a differentiation trend of CD4+ cells towards IL-4-producing cells (Th2 cells) and CD25-expressing cells (Treg cells) away from IFN-γ-producing cells (Th1 cells) and IL-17-producing cells (Th17 cells) in cerebellar ataxia rats. Left panels in (**A**) and (**B**) are representative images of flow cytometric analysis. Right panels in (**A**) and (**B**) are their respective statistical graphs. *$p<0.05$, **$p<0.01$, compared with intact or saline rats.

3-AP does not alter lymphocyte viability and proliferative response to Con A in vitro

To determine whether 3-AP is toxic to lymphocytes, we performed an in vitro experiment. The trypan blue staining of lymphocytes showed that percentage of living cells was not altered by any concentrations of 3-AP used relative to that of untreated control (Figure 4C). In addition, Con A significantly increased
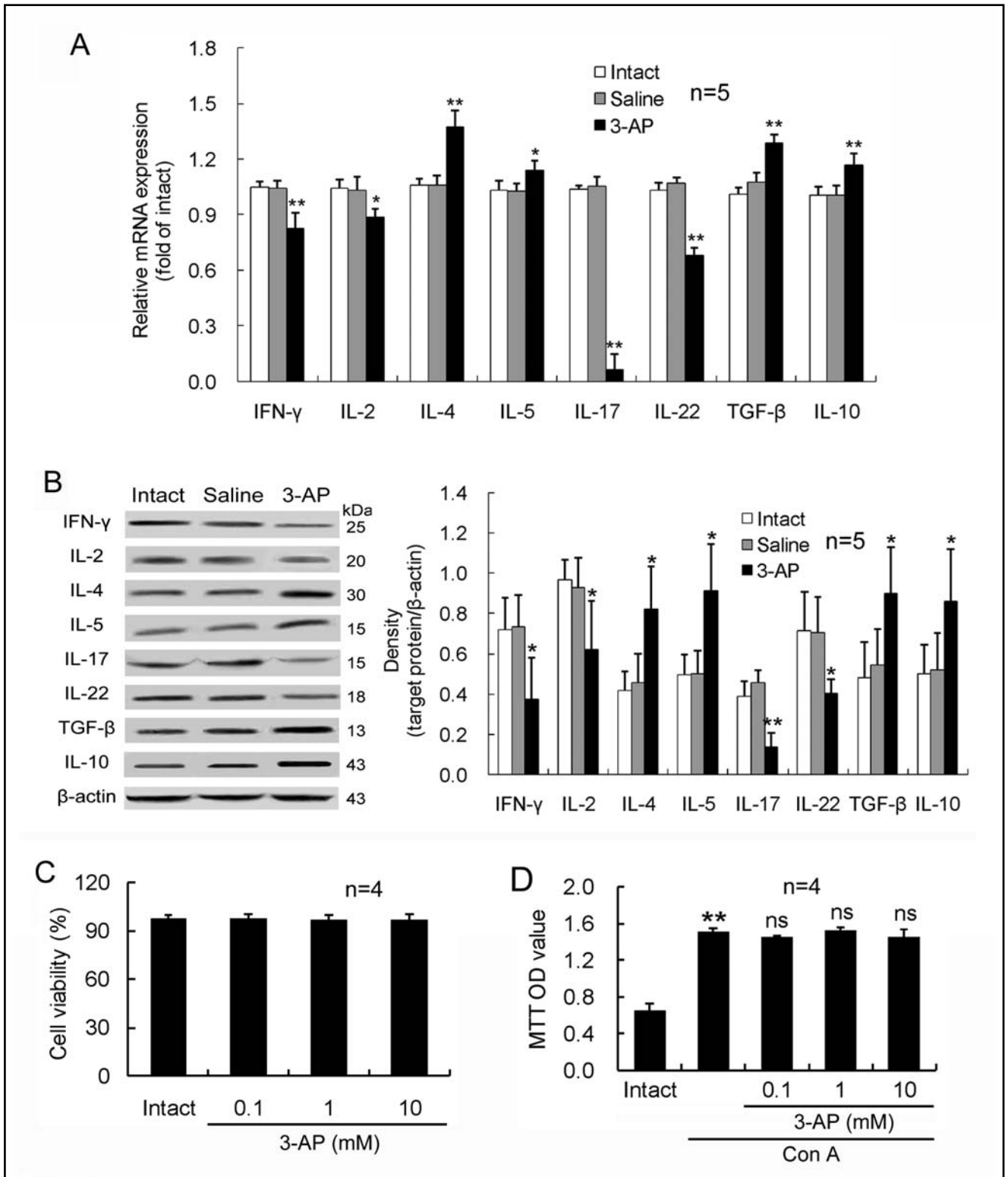
Fig. 4. Th1- and Th17-related cytokines are downregulated but Th2- and Treg-related cytokines are upregulated in CD4+ cells in cerebellar ataxia rats. On the 7th day after intraperitoneal injection of 3-AP, CD4+ cells were purified from the mesenteric lymph nodes and incubated with anti-rat CD3/CD28 for 72 h. The gene and protein expression levels for Th1 cytokines (IFN-γ and IL-2), Th2 cytokines (IL-4 and IL-5), Th17 cytokines (IL-17 and IL-22), and Treg cytokines (TGF-β and IL-10) in CD4+ T cells are shown in (**A**) and (**B**), respectively. *$p<0.05$, **$p<0.01$, compared with intact or saline-treated rats. (C) and (D) show that 3-AP does not alter lymphocyte viability and proliferative response. Lymphocytes were isolated from the mesenteric lymph nodes and treated with 3-AP for 48 h. Trypan blue staining indicates that living cells account for about 97% in total cells, regardless of with or without 3-AP treatment (C). MTT OD value shows that lymphocytes have a proliferative response to Con A and this response is not altered by any concentrations of 3-AP used (D). **$p<0.01$, compared with intact control; ns, no significance compared with Con A treatment alone.

MTT OD value of lymphocytes. This proliferative response of lymphocytes to Con A was not affected by the concentrations of 3-AP with respect to that of cells untreated by 3-AP (Figure 4D).

Cerebellar ataxia model rats are enhanced in B lymphocyte number and function

Percentage of CD3⁻CD45RA⁺ cells (B lymphocytes) in PBMCs was higher in 3-AP-induced cerebellar ataxia rats than in intact or saline rats (Figure 5A). After immunization with BSA, the cerebellar ataxia rats produced more anti-BSA IgM and IgG antibodies in serum than intact or saline animals (Figure 5B).

DISCUSSION

In this study, 3-AP intraperitoneal injection led to impairments in behavior and motor coordination. Further, Nissl staining showed that 3-AP induced neuronal loss in all the three cerebellar nuclei, FN, IN and DN. In addition, a decrease in contents of glutamate and GABA, but not glycine, was observed in the three cerebellar nuclei after 3-AP injection. These data confirm an establishment of cerebellar ataxia rat model and also demonstrate that glutamatergic and GABAergic neurons whose somas or axonal terminals are located in the three cerebellar nuclei are involved in the 3-AP-induced cerebellar ataxia. More importantly, the 3-AP injection resulted in a shift in differentiation and function of CD4⁺ cells from Th1 and Th17 cells towards Th2 and Treg cells. But 3-AP was not toxic to lymphocytes as determined by an unchanged lymphocyte viability and proliferation. Moreover, B cell number and anti-BSA antibody response were enhanced by the 3-AP injection. These findings for the first time establish that cerebellar ataxia alters immunological properties.

3-AP intraperitoneal injection has been classically used to induce a rat model of cerebellar ataxia (Fernandez *et al.* 1998; Wecker *et al.* 2013). Our present results support these reports and provide further evidence by showing that 3-AP leads to neuronal loss and neurotransmitter decrease in cerebellar nuclei. Since 3-AP directly and selectively destroys the inferior olive nucleus, the damage to the cerebellar nuclei is an outcome of losing innervations and supports from climbing fibers of the inferior olive nucleus. The climbing fibers form synapses on Purkinje cells that project axons to all three cerebellar nuclei and use GABA as neurotransmitter. Therefore, the GABA decrease in the three cerebellar nuclei is a major outcome for the indirect injury to Purkinje cells by 3-AP. Purkinje cells are the only neurons that export information from the cerebellar cortex to cerebellar nuclei. They form synapses on glutamatergic neurons in cerebellar nuclei (Nakanishi 2009). Therefore, the glutamate decrease in the three cerebellar nuclei may also be caused by the indirect injury to Purkinje cells by 3-AP. These results explain a mechanism by which 3-AP leads to cerebel-
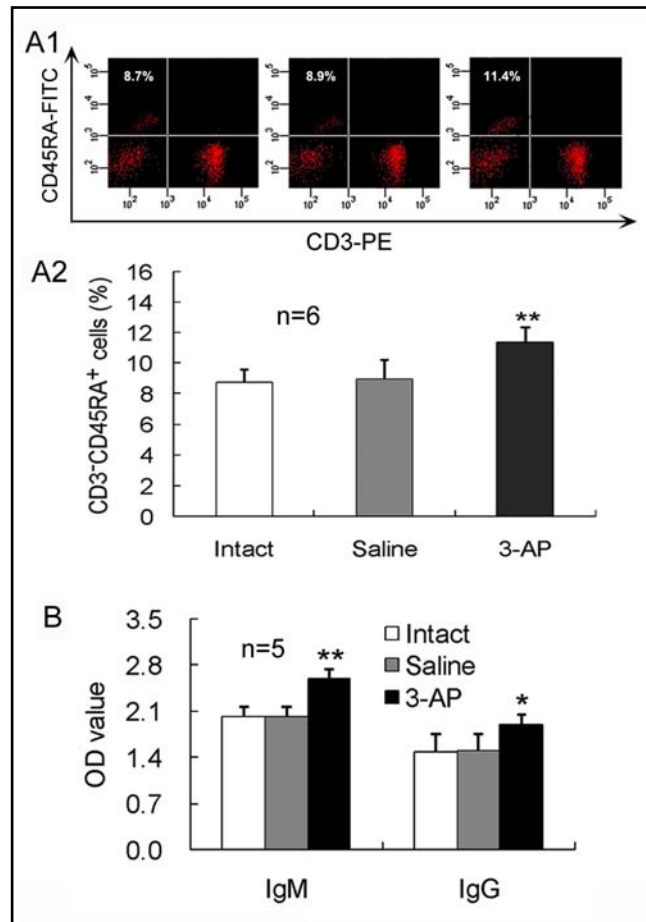

Fig. 5. B lymphocytes are enhanced in number and function in cerebellar ataxia rats. (**A1**) A representative image showing percentage of B lymphocytes (CD3⁻CD45RA⁺ cells) in PBMCs by flow cytometric analysis. (**A2**) A statistical histogram for the percentage of CD3⁻CD45RA⁺ cells. (**B**) IgM and IgG antibody levels in the serum of the rats that had been immunized with BSA. The anti-BSA IgM and IgG antibody levels were determined on day 5 (a peak period for IgM antibody response) and on day 10 (a peak period for IgG antibody response) after immunization, respectively. *$p<0.05$, **$p<0.01$, compared with intact or saline-treated rats.

lar ataxia and also identify a nerve pathway destroyed by 3-AP: the inferior olive nucleus–Purkinje cells–cerebellar nuclei. The behavioral and motor coordination impairments after 3-AP injection also confirm the establishment of cerebellar ataxia model.

Importantly, the cerebellar ataxia was accompanied by T and B cell immunological changes. In T lymphocytes (CD3⁺ cells), the subset CD4⁺ cells, but not CD8⁺ cells, were increased in percentage. CD4⁺ cells are principally subdivided into the four subpopulations, Th1, Th2, Th17 and Treg cells, which express cytokines IFN-γ, IL-4, IL-17 or CD molecule CD25, respectively. We found that both IFN-γ-producing cells and IL-17-producing cells were decreased in cerebellar ataxia rats, while both IL-4-producing cells and CD25-expressing cells were increased. These data suggest that CD4⁺ cell differentiation in cerebellar ataxia rats has a shift from Th1 and Th17 cells towards Th2 and Treg cells. In sup-

port of these data, the expression of both the Th1-related cytokines, IFN-γ and IL-2, and the Th17-related cytokines, IL-17 and IL-22, was downregulated, whereas the expression of both the Th2-related cytokines, IL-4 and IL-5, and the Treg-related cytokines, TGF-β and IL-10, was upregulated in CD4+ cells in cerebellar ataxia rats. These findings strongly show that Th1 and Th17 cells are attenuated but Th2 and Treg cells are enhanced in differentiation and function in cerebellar ataxia rats. Th1 and Th17 cells have been identified to promote cellular immunity and pro-inflammatory response, and Th2 and Treg cells are involved in mediation of humoral immunity and anti-inflammatory response. Thus, the present results suggest that cerebellar ataxia is accompanied by a reduced cellular immunity and pro-inflammatory response and an enhanced humoral immunity and anti-inflammatory response. As a support, both the number of B cells and the levels of anti-BSA IgM and IgG antibodies were elevated in cerebellar ataxia rats. These data further demonstrate that an enhanced humoral immune response occurs in cerebellar ataxia.

In our recent work, we have shown that cerebellar FN and IN are involved in modulation of the immune system (Lu *et al.* 2012; Cao *et al.* 2012, 2013; Xu *et al.* 2014). Therefore, it is easily understood that the damage to the cerebellum by 3-AP causes immunological changes. To exclude the possibility of 3-AP injury directly to lymphocytes, we performed an additional in vitro experiment. These results showed that lymphocyte viability and proliferative response to Con A were not altered by 3-AP treatment. Combining the in vitro data with the in vivo results showing that T and B lymphocytes in blood were increased rather than decreased by 3-AP treatment, we confirm that 3-AP is not directly toxic to peripheral lymphocytes. This viewpoint is supported by the reports presenting that neuronal cells are almost completely lost while non-neuronal cells are less affected by 3-AP (Weller *et al.* 1992; Wüllner *et al.* 1997). Thus, we propose that the immunological changes occurring in 3-AP-induced cerebellar ataxia are a subsequent outcome due to the lesions to the cerebellum. However, the role and significance of the immunological changes in cerebellar ataxia are still unclear. Interestingly, Melzer *et al.* (2012) reported that in a single case the patient with pronounced cerebellar atrophy and hypometabolism shows that both B cells and CD8+ T cells are preferentially recruited to and activated within cerebrospinal fluid, suggesting that cerebellar ataxia may be an inflammatory central nervous system disease. Recently, accumulated evidence has shown that inflammation is involved in neurodegenerative diseases such as Alzheimer's disease and Parkinson's disease (Qian *et al.* 2010; González & Pacheco 2014; Varley *et al.* 2014). Here, we provide more evidence for the involvement of the immune system in cerebellar ataxia, a neurodegenerative disease. Nevertheless, the significance and mechanism of immunological changes in cerebellar ataxia need clarification in the future to better understand these phenomena and to develop therapeutic strategies for cerebellar ataxia.

ACKNOWLEDGEMENTS

REFERENCES

1 Abbasi S, Edrisi M, Mahnam A, Janahmadi M (2013). Computational insights into the neuroprotective action of riluzole on 3-acetylpyridine-induced ataxia in rats. Cell J. **15**: 98–107.
2 Aoki H, Sugihara I (2012). Morphology of single olivocerebellar axons in the denervation-reinnervation model produced by subtotal lesion of the rat inferior olive. Brain Res. **1449**: 24–37.
3 Brusse E, Maat-Kievit JA, van Swieten JC (2007). Diagnosis and management of early-and late-onset cerebellar ataxia. Clin Genet. **71**: 12–24.
4 Cao BB, Han XH, Hang Y, Qiu YH, Peng YP (2012). The hypothalamus mediates the effect of cerebellar fastigial nuclear glutamatergic neurons on humoral immunity. Neuro Endocrinol Lett. **33**: 393–400.
5 Cao BB, Hang Y, Lu JH, Xu FF, Qiu YH, Peng YP (2013). Cerebellar fastigial nuclear GABAergic projections to the hypothalamus modulate immune function. Brain Behav Immun. **27**: 80–90.
6 Desclin JC, Escubi J (1974). Effects of 3-acetylpyridine on the central nervous system of the rat, as demonstrated by silver methods. Brain Res. **77**: 349–364.
7 Driessen GJ, ljspeert H, Weemaes cm, Haraldsson A, Trip M, Warris A, et al. (2013). Antibody deficiency in patient with ataxia telangiectasia is caused by disturbed B- and T-cell homeostasis and reduced immune repertoire diversity. J Allergy Clin Immunol. **131**: 1367–1375.
8 Fernandez AM, de la Vega AG, Torres-Aleman I (1998). Insulin-like growth factor restores motor coordination in a rat model of cerebellar ataxia. Proc Natl Acad Sci USA. **95**: 1253–1258.
9 Ghoshal D, Sinha S, Sinha A, Bhattacharyya P (1998). Immunosuppressive effect of vestibulo-cerebellar lesion in rats. Neurosci Lett. **257**: 89–92.
10 González H, Pacheco R (2014). T-cell-mediated regulation of neuroinflammation involved in neurodegenerative diseases. J Neuroinflammation. **11**: 201.
11 Green-Johnson JM, Zalcman S, Vriend CY, Nance DM, Greenberg AH (1995). Suppressed T cell and macrophage function in the "reeler"(rl/rl) mutant, a murine strain with elevated cerebellar norepinephrine concentration. Brain Behav Immun. **9**: 47–60.
12 Janahmadi M, Goudarzi I, Kaffashian MR, Behzadi G, Fathollahi Y, Hajizadeh S (2009). Co-treatment with riluzole, a neuroprotective drug, ameliorates the 3-acetylpyridine-induced neurotoxicity in cerebellar Purkinje neurons of rats: behavioural and electrophysiological evidence. Neurotoxicology. **30**: 393–402.
13 Llinás R, Walton K, Hillman DE, Sotelo C (1975). Inferior olive: its role in motor learning. Science. **190**: 1230–1231.
14 Lu JH, Mao HN, Cao BB, Qiu YH, Peng YP (2012). Effect of cerebellohypothalamic glutamatergic projections on immune function. Cerebellum. **4**: 905–916.
15 Marmolino D, Manto M (2010). Past, present and future therapeutics for cerebellar ataxias. Curr Neuropharmacol. **8**: 41–61.
16 Melzer N, Golombeck KS, Gross CC, Meuth SG, Wiendl H (2012). Cytotoxic CD8+ T cells and CD138+ plasma cells prevail in cerebrospinal fluid in non-paraneoplastic cerebellar ataxia with contactin-associated protein-2 antibodies. J Neuroinflammation. **9**: 160.

17 Mori RL, Cotter LA, Arendt HE, Olsheski CJ, Yates BJ (2005). Effects of bilateral vestibular nucleus lesions on cardiovascular regulation in conscious cats. J Appl Physiol. **98**: 526–533.

18 Nakanishi S (2009). Genetic manipulation study of information processing in the cerebellum. Neuroscience. **162**: 723–731.

19 ⬚Paxinos G, Watson C (2007). The Rat Brain in Stereotaxic Coordinates. 6th ed. Amsterdam: Elsevier Academic Press.

20 Peng YP, Qiu YH, Cao BB, Wang JJ (2005). Effect of lesions of cerebellar fastigial nuclei on lymphocyte functions of rats. Neurosci Res. **51**: 275–284.

21 Peng YP, Qiu YH, Qiu J, Wang JJ (2006). Cerebellar interposed nucleus lesions suppress lymphocyte function in rats. Brain Res Bull. **71**: 10–17.

22 Qian L, Flood PM, Hong JS (2010). Neuroinflammation is a key player in Parkinson's disease and a prime target for therapy. J Neural Transm. **117**: 971–979.

23 Rosenberger C, Thürling M, Forsting M, Elsenbruch S, Timmann D, Gizewski ER (2013). Contributions of the cerebellum to disturbed central processing of visceral stimuli in irritable bowel syndrome. Cerebellum. **12**: 194–198.

24 Sierra A, Azcoitia I, Garcia-Segura L (2003). Endogenous estrogen formation is neuroprotective in model of cerebellar ataxia. Endocrine. **21**: 43–51.

25 Sivera R, Martin N, Bosca I, Sevilla T, Muelas N, Azorin I, et al. (2012). Auoimmuniy as a prognostic factor in sporadic adult onset cerebellar ataxia. J Neurol. **259**: 851–854.

26 Sugihara I (2006). Organization and remodeling of the olivocerebellar climbing fiber projection. Cerebellum. **5**: 15–22.

27 Sugihara I (2011). Bright field neuronal preparation optimized for automatic computerized reconstruction, a case with cerebellar climbing fibers. Neuroinformatics. **9**: 113–118.

28 Sugihara I, Wu HS, Shinoda Y (1999). Morphology of single olivocerebellar axons labeled with biotinylated dextran amine in the rat. J Comp Neurol. **414**: 131–148.

29 Sugihara I, Wu HS, Shinoda Y (2001). The entire trajectories of single olivocerebellar axons in the cerebellar cortex and their contribution to cerebellar compartmentalization. J Neurosci. **21**: 7715–7723.

30 Varley J, Brooks DJ, Edison P (2014). Imaging neuroinflammation in Alzheimer's and other dementias: Recent advances and future directions. Alzheimers Dement. Online: DOI 10.1016/j.jalz.2014.08.105Wecker L, Engberg ME, Philpot RM, Lambert CS, Kang CW, Antilla JC, et al. (2013). Neuronal nicotinic receptor agonists improve gait and balance in olivocerebellar ataxia. Neurophrmacology. **73**: 75–86.

31 Weller M, Marini AM, Paul SM (1992). Niacinamide blocks 3-acetylpyridine toxicity of cerebellar granule cells in vitro. Brain Res. **594**: 160–164.

32 Wen YQ, Zhu JN, Zhang YP, Wang JJ (2004). Cerebellar interpositus nuclear inputs impinge on paraventricular neurons of the hypothalamus in rats. Neurosci Lett. **370**: 25–29.

33 ⬚Wüllner U, Weller M, Groscurth P, Löschmann PA, Schulz JB, Müller I, et al. (1997). Evidence for an active type of cell death with ultrastructural features distinct from apoptosis: the effects of 3-acetylpyridine neurotoxicity. Neuroscience. **81**: 721–34.

34 Xu FF, Huang Y, Wang XQ, Qiu YH, Peng YP (2014). Modulation of immune function by glutamatergic neurons in the cerebellar interposed nucleus via hypothalamic and sympathetic pathways. Brain Behav Immun. **38**: 263–271.

35 Zhu JZ, Fei SJ, Zhang JF, Zhu SP, Liu ZB, Li TT, et al. (2012). Lateral hypothalamic area mediated the aggravated effect of microinjection of Baclofen into cerebellar fastigial nucleus on stress gastric mucosal damage in rats. Neurosci Lett. **509**: 125–129.

36 Zhu JN, Wang JJ (2008). The Cerebellum in Feeding Control: Possible Function and Mechanism. Cell Mol Neurobiol. **28**: 469–478.